Front. Electr. Electron. Eng. China 2007, 2(1): 117–122
DOI 10.1007/s11460-007-0022-y

RESEARCH ARTICLE

HUANG Jin, NIU Faliang, YANG Jiaqiang

Induction motor rotor fault diagnosis method based on double *PQ* transformation

Abstract This paper presents a new rotor fault diagnosis method for induction motors which is based on the double *PQ* transformation. We construct the *PQ* transformation matrix with the positive sequence fundamental voltage components and their Hilbert transformation as elements. The active power *P* and the reactive power *Q* are obtained through the *PQ* transformation of the stator currents. As both *P* and *Q* are constant for a healthy motor, they are represented by a dot on the *PQ* plane. Whereas the *P* and *Q* for a rotor broken bar motor are represented by an ellipse because they comprise an additional frequency component $2sf_s$ (s is the slip and f_s is the supply frequency). Thus, by distinguishing these two different patterns, the rotor broken bar fault is detected. We use the major radius of the ellipse as the fault indicator and the distance between the point of no-load condition and the center of the ellipse on the *PQ* plane as its normalization value. We thus arrive at the fault severity factor which is fairly independent of the load level and the inertia value of the induction motors. Experimental results have demonstrated that the proposed method is effective in identifying the rotor-broken-bars fault and at determining the severity of the fault.

Keywords *PQ* transformation, rotor broken bars, fault diagnosis, fault-severity factor, induction motors

1 Introduction

As driving devices, induction motors are widely used in industrial and agricultural production, because of their robustness and low cost. However, sometimes, manufacturing and assembly defects lead to the improper fixing of the rotor bars. In such cases, the vibration of the rotor bars increase due to the electromagnetic and eccentric forces in play when the motor operates under a heavy load, starts or brakes frequently. This results in cracked or broken bars especially in large induction motors, such as the coal-transported motor in the thermoelectric plant. Moreover the fatigue stresses of the adjacent bars increase if the motor with the broken bars continues to be operated, further aggravating the fault. It is further possible for the rotor-stator rub to develop with consequential damage to the core and windings and the rotor cages. Therefore, it becomes important to diagnose the rotor broken bar fault at the very inception, since unscheduled machine downtimes can upset deadlines and cause heavy financial losses.

In an induction motor with rotor broken bars fault, specific harmonic components at frequencies $f_{br} = (1 \pm 2ks)f_s$ appear in the stator current spectrum [1−10], where f_s is the supply frequency, s is the slip of the motor, and $k = 1, 2, \ldots, n$. A common approach to the diagnosis of the rotor broken bars is based on the analysis of the stator current spectrum. The amplitude of the associated spectra component can be used to evaluate the fault's severity. However, the slip for a typical cage induction motor under rated conditions is small. This means that the fault characteristic frequency of $(1 \pm 2s)f_s$ is very close to the supply frequency. As a result, the fault characteristic frequency is almost always submerged by the fundamental component, which makes the fault diagnosis that much more difficult. This proves to be a bottleneck in the rotor broken bars fault diagnosis for induction motors [2−10]. In order to avoid the influence of the spectrum leakages of the fundamental component, Cruz S. M. A. et al., had proposed solutions known as the Park vector and the extended Park vector methods [4−7]. The former, transforms the spectrum analysis into a recognizable graphics pattern. But then, making a diagnosis from the pattern is a matter of distinguishing between a circle and an ellipse, which can be difficult at the initial fault stage. The latter, introduced new frequency components because of the effect of the square operator. Despite these disadvantages, the authors had developed a new diagnostic technique which was based on the multiple reference frames theory [8]. However, a precise value of the supply frequency must first be given, which is difficult when

Translated from *Proceedings of the Chinese Society for Electrical Engineering*, 2006, 26(13): 135–140 [译自: 中国电机工程学报]

HUANG Jin, NIU Faliang, YANG Jiaqiang (✉)
College of Electrical Engineering, Zhejiang University,
Hangzhou 310027, China
E-mail: yjq1998@163.com

the supply quality is poor. Utilizing modern signal processing techniques such as wavelet analysis, Hilbert-Huang transformation and others, researchers have attempted to investigate the startup or breakdown process of induction motors [9−10]. However, these methods have not proved to be successful in all cases. Moreover, the appropriate expression for the fault severity has not been defined so far.

We present in this paper a new method for rotor broken bar fault diagnosis for induction motors based on the double *PQ* transformation as a solution to this technical puzzle. The paper presents the theory of double *PQ* transformation and the rotor fault diagnosis technique under stable operations, which not only overcomes the drawbacks of the spectral analysis and the difficulty of graphic pattern recognition based on the Park vector analysis, but also avoids computation of the supply frequency for the multiple reference transformation. The proposed method is furthermore not affected by the vibration of the supply frequency. The major radius of the ellipse is used as the fault indicator, and the distance between the point of no-load condition and the center of the ellipse on the *PQ* reference coordinates is taken as its normalization value, to determine the fault severity factor which is fairly independent of the load level and the inertia value of the induction motors.

2 *PQ* transformation

2.1 Problems with the synchronous reference frame transformation method

The transformation matrix from the stationary three-phase *abs* to the synchronous $d_c q_c 0$ reference frame can be expressed as

$$\boldsymbol{C}_{d_c,q_c}^{a,b,c}=\sqrt{\frac{2}{3}}\begin{bmatrix}\cos\theta & \cos\left(\theta-\frac{2\pi}{3}\right) & \cos\left(\theta+\frac{2\pi}{3}\right)\\ -\sin\theta & -\sin\left(\theta-\frac{2\pi}{3}\right) & -\sin\left(\theta+\frac{2\pi}{3}\right)\end{bmatrix} \quad (1)$$

where $\theta=\omega_s t+\theta_0$ is the angle between *d*-axis and *a*-axis, θ_0 is the angle at $t=0$ and $\omega_s=2\pi f_s$. For simplicity, the zero sequence components have been left out in this paper. When transforming the stationary current from the stationary three-phase *abc* to the synchronous $d_c q_c 0$ reference frame, the fundamental positive sequence current components appear as direct current components in i_{d_c} and i_{q_c} components. The frequency of the fault feature components are transformed to $2ksf_s$. But, it is difficult to derive the accurate value of the supply frequency because it keeps fluctuating. If there is an error Δf_s, between the actual frequency and the calculated value, the harmonic component at the frequency of Δf_s will be introduced into the components i_{d_c} and i_{q_c}. On the other hand, because the rated slip is only approximately 0.5%−5% for large induction motors, the fault feature frequency $2ksf_s$ is about 0.5−5 Hz when $k=1$. Therefore, the fault feature components tend to be mixed with the harmonic component due to the predicted error in the supply frequency, thereby making reliable fault diagnosis difficult.

2.2 Definition of the *PQ* transformation

The ideal balanced supply voltage in the *abc* reference frame can be expressed as

$$\begin{cases}u_a=\sqrt{2}U\cos\ (\omega_s t)\\ u_b=\sqrt{2}U\cos\ \left(\omega_s t-\frac{2\pi}{3}\right)\\ u_c=\sqrt{2}U\cos\ \left(\omega_s t+\frac{2\pi}{3}\right)\end{cases} \quad (2)$$

where $\sqrt{2}U$ refers to the magnitude of the voltages. When these voltages act upon a healthy motor, the ensuing stator currents are defined as

$$\begin{cases}i_a=\sqrt{2}I\cos\ (\omega_s t-\alpha_I)\\ i_b=\sqrt{2}I\cos\ \left(\omega_s t-\alpha_I-\frac{2\pi}{3}\right)\\ i_c=\sqrt{2}I\cos\ \left(\omega_s t-\alpha_I+\frac{2\pi}{3}\right)\end{cases} \quad (3)$$

where $\sqrt{2}I$ and α_I refer to the magnitude and the phase angle respectively. Obviously, the value of u_a, u_b and u_c can be used to substitute the elements of the first row in Eq. (1). Moreover, since the equation of a sinusoidal waveform shifted by π/2 backward is given by its Hilbert transformation [11], the elements of the second row in Eq. (2) are obtained by performing the Hilbert transformation on u_a, u_b and u_c respectively. Consequently, a new matrix $\hat{C}_{d_c,q_c}^{a,b,c}$ is defined as

$$\hat{\boldsymbol{C}}_{d_c,q_c}^{a,b,c}=\begin{bmatrix}u_a & u_b & u_c\\ -H(u_a) & -H(u_b) & -H(u_c)\end{bmatrix} \quad (4)$$

where H is the Hilbert operator. If the initial phase angle of the *a* phase voltage is used as the angle between d_c and *a*-axis, the relationship between Eqs. (4) and (1) becomes $\hat{C}_{d_c,q_c}^{a,b,c}/C_{d_c,q_c}^{a,b,c}=\sqrt{3}U$.

Then, after performing transformation on the stator currents based on $\hat{C}_{d_c,q_c}^{a,b,c}$, the d_c, q_c current components are represented by

$$\begin{bmatrix}i_{d_c}\\ i_{q_c}\end{bmatrix}=\hat{C}_{d_c,q_c}^{a,b,c}\begin{bmatrix}i_a\\ i_b\\ i_c\end{bmatrix}=3UI\begin{bmatrix}\cos\alpha_I\\ -\sin\alpha_I\end{bmatrix}=\begin{bmatrix}P\\ -Q\end{bmatrix} \quad (5)$$

The value of active power P and the negative value of the reactive power Q are obtained from Eq. (4). Consequently, we define the transformation of the stator currents based on $\hat{C}_{d_c,q_c}^{a,b,c}$ as the PQ transformation, which avoids calculation of the supply frequency.

Exchanging the elements of the second and third columns in Eq. (4), the counterclockwise PQ transformation matrix can be written as

$$\bar{C}_{d_c,q_c}^{a,b,c}=\begin{bmatrix} u_a & u_c & u_b \\ -H(u_a) & -H(u_c) & -H(u_b) \end{bmatrix} \tag{6}$$

2.3 Extraction of the fundamental positive sequence components of the supply voltage

The voltages of u_a, u_b and u_c in Eq. (4) are the fundamental positive sequence components of the supply voltage. However, the supply voltage also contains the negative sequence and the harmonics components. This makes the PQ transformation matrix complicated [12−14]. Therefore, the fundamental positive sequence components of the supply voltage need to be first extracted in order to eliminate the unwanted harmonics in the PQ components.

A low-pass digital filter is to be used to eliminate the high harmonics in the supply voltage. Thereafter the supply voltage will only comprise of the positive and the negative sequence fundamental components, which is expressed as

$$\begin{cases} u_a=\sqrt{2}[U^+\cos\ (\omega_s t+\phi_u^+)+U^-\cos\ (\omega_s t\ +\ \phi_u^-)] \\ u_b=\sqrt{2}\left[U^+\cos\ \left(\omega_s t+\phi_u^+-\dfrac{2\pi}{3}\right)\right. \\ \qquad \left.+U^-\cos\ \left(\omega_s t\ +\ \phi_u^-+\dfrac{2\pi}{3}\right)\right] \\ u_c=\sqrt{2}\left[U^+\cos\ \left(\omega_s t+\phi_u^++\dfrac{2\pi}{3}\right)\right. \\ \qquad \left.+U^-\cos\ \left(\omega_s t+\phi_u^--\dfrac{2\pi}{3}\right)\right] \end{cases} \tag{7}$$

where $\sqrt{2}U^+$, $\sqrt{2}U^-$, ϕ_u^+ and ϕ_u^- are the magnitude and the phase angle of the positive and the negative sequence fundamental voltage components respectively. Then the α, β voltage components are

$$\begin{cases} v_\alpha=\sqrt{3}[U^+\cos\ (\omega_s t+\phi_u^+)+U^-\cos\ (\omega_s t+\phi_u^-)] \\ \quad =v_\alpha^++v_\alpha^- \\ v_\beta=\sqrt{3}[U^+\sin\ (\omega_s t+\phi_u^+)-U^-\sin\ (\omega_s t+\phi_u^-)] \\ \quad =v_\beta^++v_\beta^- \end{cases} \tag{8}$$

We perform the Hilbert transformation on v_α and v_β in Eq. (8) respectively. The fundamental positive sequence components in the α, β reference frame is now calculated by

$$\begin{cases} v_\alpha^+=\dfrac{1}{2}[v_\alpha-H(v_\beta)] \\ v_\beta^+=\dfrac{1}{2}[v_\beta+H(v_\alpha)] \end{cases} \tag{9}$$

where v_α^+ and v_β^+ are the fundamental positive sequence components of the supply voltage in the α,β reference frames respectively. Thereafter, the fundamental positive sequence components of the supply voltage can be obtained through the reverse transformation of the α, β reference frames.

3 Rotor broken bar fault diagnosis based on double *PQ* transformation

3.1 Elimination of the negative sequence current components based on the reverse *PQ* transformation

The high order harmonics in the stator currents are to be eliminated similarly as described earlier in the case of the supply voltages. However, the negative sequence components in the stator current appear because of the inherent asymmetry of the induction motor and the supply voltages. This results in 2nd order harmonic of the supply current in the PQ components, which also makes the rotor fault diagnosis difficult. Therefore, the negative sequence current components need to be eliminated before performing the rotor broken bar fault diagnosis.

After filtering the current with a low pass filter, the stator currents for a healthy motor are expressed as

$$\begin{cases} i_a=\sqrt{2}[I^+\cos\ (\omega_s t-\phi_i^+)+I^-\cos\ (\omega_s t-\phi_i^-)] \\ i_b=\sqrt{2}\left[I^+\cos\ \left(\omega_s t-\phi_i^+-\dfrac{2\pi}{3}\right)+I^-\cos\ \left(\omega_s t-\phi_i^-+\dfrac{2\pi}{3}\right)\right] \\ i_c=\sqrt{2}\left[I^+\cos\ \left(\omega_s t-\phi_i^++\dfrac{2\pi}{3}\right)+I^-\cos\ \left(\omega_s t-\phi_i^--\dfrac{2\pi}{3}\right)\right] \end{cases} \tag{10}$$

where $\sqrt{2}I^+$, $\sqrt{2}I^-$, ϕ_i^+ and ϕ_i^- are the magnitude and phase of the positive and negative sequence fundamental current components, respectively. After performing the counterclockwise PQ transformation on the current components in Eq. (10), I^+ translates twice the fundamental supply frequency components and I^- translates a DC component in P, which should be filtered from them. The stator current is then to be calculated through the reverse PQ transformation, after filtering the negative sequence current components.

3.2 Extraction of the rotor broken bar fault feature

It can be concluded from Eq. (5), that both the P and Q components for a healthy motor are constant. If we define the PQ coordinate using the P and Q components as the coordinate axes, the locus of the P, Q components for the healthy motor

will correspond to a dot. But for the motor with rotor broken bar, its stator currents contain the left and right side band components. And i'_a is defined as

$$i'_a = \sqrt{2}I\cos\ (\omega_s t-\alpha_I)+\sqrt{2}I_1\cos\ [(1-2s)\omega_s t-\alpha_1] + \sqrt{2}I_r\cos\ [(1+2s)\omega_s t-\alpha_r] \quad (11)$$

where $\sqrt{2}I_1$ $\sqrt{2}I_r$, α_1 and α_r are the magnitude and phase of the left and right side band current components respectively.

We perform the PQ transformation in Eq. (11) as follows

$$\begin{bmatrix}P'\\Q'\end{bmatrix}= \hat{C}^{a,b,c}_{d_c,q_c}\begin{bmatrix}i'_a\\i'_b\\i'_c\end{bmatrix}=\begin{bmatrix}P\\-Q\end{bmatrix} +3U\begin{bmatrix}I_1\cos\ (2s\omega_s t+\alpha_1)+I_r\cos\ (2s\omega_s t-\alpha_r)\\-I_1\sin\ (2s\omega_s t+\alpha_1)+I_r\sin\ (2s\omega_s t-\alpha_r)\end{bmatrix} \quad (12)$$

Equation (12) shows that the PQ components contain a DC component plus an additional component at twice of the rotor slip frequency when the rotor broken bar fault occurs. Predictably, the locus in the PQ plane is an elliptic pattern. The coordinates of the ellipse center are the dc values, and its major and minor axis are $3U(I_1+I_r)$ and $3U(I_1-I_r)$ respectively. Consequently, the rotor broken bar fault is detected by identifying the ellipse in the PQ plane, as shown in Fig. 1. The proposed fault diagnosis method, called the double PQ transformation, applies the reverse to eliminate the negative sequence current components and performs the PQ transformation to detect the rotor broken bars fault.

3.3 Evaluation of rotor fault severity factor

In Ref. [15], the sum of the left and right side band components amplitude constitutes the fault factor which is independent of the motor inertia and is proportional to the major radius of the ellipse in the PQ plane. Therefore, the major axis of the ellipse R_f is taken as the rotor broken bar fault factor, as shown in Fig. 1.

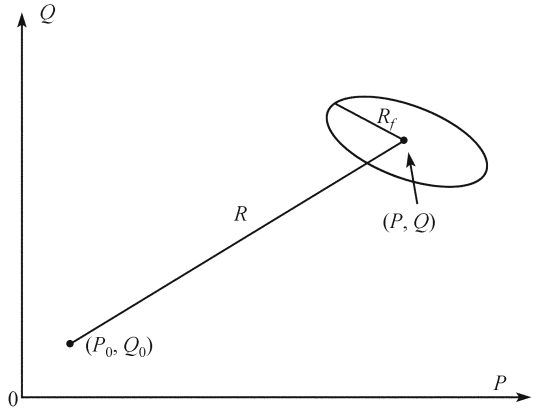

Fig. 1 Definition of the rotor fault severity factor

In particular, when motors operate under small or no load conditions, the copper loss and the stator core loss play a large role in the input power, which represents the no-load power, and are irrelevant to the rotor fault [16−17]. Therefore, the distance between the point of no-load condition and the center of the ellipse on the PQ plane is taken as normalization to gain the rotor fault factor δ, as

$$\delta = \frac{R_f}{R} \quad (13)$$

From the above analysis, we deduce that the fault factor δ, which represents the rotor fault severity, is independent of the load level and the motor inertia.

4 Diagnosis example

4.1 Experiment system

The main parameters of the test induction machine are shown in Table 1. To test the applicability of the proposed diagnostic techniques for the diagnosis of the rotor broken bars, a special test motor is used. A set of additional cage rotors fabricated with the following faults—one rotor broken bar, two-adjacent rotor broken bars—are used in the test. The test motor is star-connected and without a neutral line. A coaxial separately-excited DC generator is used as the load for the test motor. The terminal data u_{ab}, u_{cb}, i_a and i_c for the line-connected motor are gathered. The voltages and currents of the induction motor are represented by

$$i_b = -(i_a+i_c) \quad (14)$$

$$\begin{bmatrix}u_a\\u_b\\u_c\end{bmatrix}=\frac{1}{3}\begin{bmatrix}1&0&-1\\-1&1&0\\0&-1&1\end{bmatrix}\begin{bmatrix}u_{ab}\\u_{bc}\\u_{ca}\end{bmatrix}=\frac{1}{3}\begin{bmatrix}2u_{ab}-u_{cb}\\-u_{ab}-u_{cb}\\-u_{ab}+2u_{cb}\end{bmatrix} \quad (15)$$

Table 1 Specifications of the test motor

Rated power /kW	Rated voltage /V	Rated current /A	Rated speed /(r·min^{-1})	Rotor bar /number
4	380	10	1 400	32

The sample frequency is 10 kHz. A pre-filter whose cut-off frequency satisfies the Shannon sample theorem is used to avoid the collapse of the high frequency components. The same low pass digital filter is used to filter the high frequency components in the sample data.

4.2 Results and analysis

The PQ locus, for the healthy motor as well as the ones for the one and the two adjacent rotor broken bars motors, when the motors are operated under the rated load conditions in the PQ

plane, are shown in Figs. 2, 3 and 4 respectively. Figure 2 shows that the PQ components are basically constant; that is, their representation in the PQ plane is a point. However, Figs. 3 and 4 indicate that if the motor has a rotor broken bar, the representation of its PQ components is an ellipse in the PQ plane. The major and minor axes in Fig. 4 for the two adjacent rotor broken bars motor are longer than those in Fig. 3 for the one rotor broken bar motor. This demonstrates that the fault in the two rotor broken bars motor is more severe.

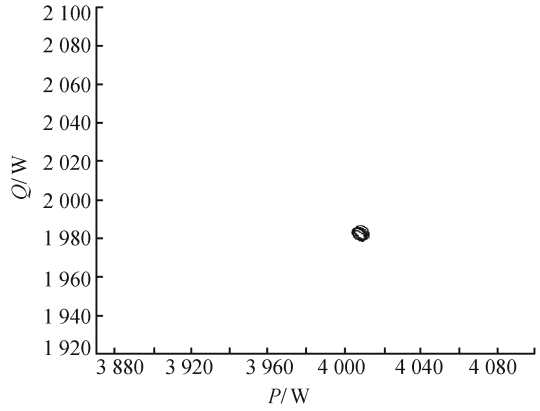

Fig. 2 PQ of the healthy motor

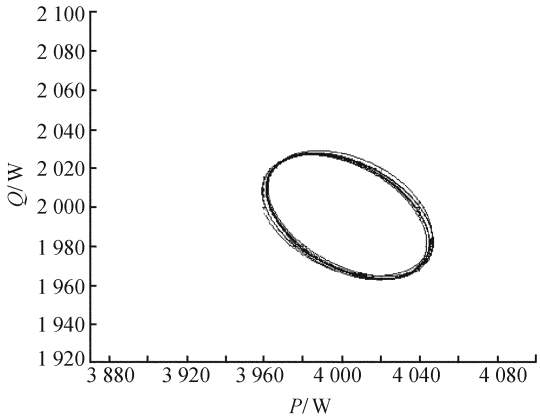

Fig. 3 PQ of the one rotor broken bar motor

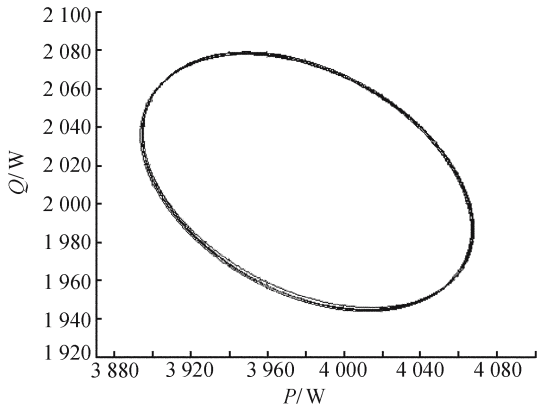

Fig. 4 PQ of the two adjacent rotor broken bars motor

The computation results of Eq. (13), when the motors are operated with the rated load are presented in Table 2. The results show that the rotor fault factor increases linearly with respect to the number of broken bars; thus, they validate the definition of the rotor fault factor δ.

Table 2 Computation of the rotor fault severity factor δ

Condition	Ellipse center (P, Q)	No-load point (P_0, Q_0)	R/W	R_f/W	δ/%
The healthy	(3 976.0, 1 956.0)	(243.4, 932.3)	3 870.4	2.3	0.06
1 broken bars	(4 003.0, 1 994.8)	(242.3, 915.6)	3 913.2	47.0	1.20
2 broken bars	(3 979.0, 2 010.0)	(230.5, 931.0)	3 900.0	95.0	2.44

Figure 5 presents the relationship between the rotor fault factor δ and the load level. We can see that the calculated fault severity factor increases slightly with the increase in the load level and is fairly independent of the load level.

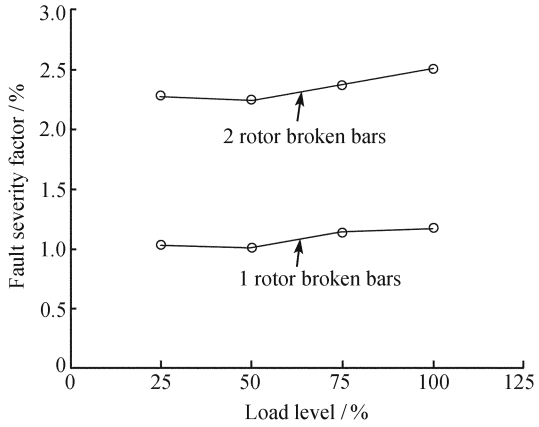

Fig. 5 Fault-severity factor versus load-level of the rotor broken bars motor

5 Conclusions

The paper proposes a new rotor-broken-bar fault diagnosis method for induction motors based on the double PQ transformation. The rotor broken bar fault can be detected by identification of the patterns of the PQ components in the PQ plane. The proposed method avoids the burden of computing the supply frequency value, which is influenced by the quality of the supply. The method not only overcomes the drawbacks of the spectral analysis and the difficulty of recognition of graphics based on the Park Vector analysis, but also avoids computation of the supply frequency in the multiple reference transformation. In other words, the proposed method is not affected by the vibration of the supply frequency. The fault severity factor, which is fairly independent of the load level and the inertia value of the motors, is determined by using the major radius of the ellipse as the fault indicator and the distance between the point of no-load condition and the center of the ellipse on the PQ reference

coordinates as its normalization value. Experimental results prove the effectiveness of the proposed method.

Acknowledgements This work was supported by the National Natural Science Foundation of China (Grant No. 50307011), Many acknowledgements are to Nanjing Nanzi Electric-mechanical Automation Co. Ltd for its fund and Zhejiang Wolong Electric Group for its test motor.

References

1. Ethan Y, Song Y H. Condition monitoring techniques for electrical equipment-a literature survey. IEEE Trans. Power Delivery, 2003, 18(1): 4−13
2. Liu Zhenxing, Yin Xianggen, Zhang Zhe. On-line monitoring and diagnosis way based on spectrum analysis of Hilbert modulus in induction motors. Procedings of the CSEE, 2003, 23(7): 158−161 (in Chinese)
3. Xu Boqiang, Li Heming, Sun Liling, et al. A novel detection method for broken rotor bars in induction motors. Proceedings of the CSEE 2004, 24(5): 115−119 (in Chinese)
4. Cruz S M A., Cardoso A J M., Carvalho J F S, et al. Rotor cage fault diagnosis in three-phase induction motors by Park's vector approach. In: Conference Record of the 1995 IEEE Industry Applications Society Annual Meeting. Orland Florida: 1995, 1: 642−646
5. Cruz S M A, Cardoso A J M. Rotor cage fault diagnosis in three-phase induction motors by extend Park's vector approach. Electric Machines and Power Systems, 2000, 28 (3): 289−299
6. Cruz S M A, Cardoso A J M. Stator winding fault diagnosis in three-phase synchronous and asynchronous motors by the extended Park's vector approach. IEEE Trans. Ind. 2001, 37(5): 1227−1233
7. Hou Xinguo, Wu Guozheng, Xia Li. A method for detecting rotor faults in asynchronous motors based on the square of the Park's vector modulus. Proceedings of the CSEE, 2003, 23(9): 137−140 (in Chinese)
8. Cruz S M A, Cardoso A J M, Toliyat H A. Diagnosis of stator rotor and airgap eccentricity faults in three-phase induction motors based on the multiple reference frames theory. In: Conference Record of The 2003 IEEE Industry Applications Society Annual Meeting. Salt Lake City: 2003, 2: 1340−1346
9. Niu Faliang, Huang Jin, Yang Jiaqiang, et al. Rotor broken-bar fault diagnosis of induction motor based on Hilbert-Huang transformation of the startup electromagnetic torque. Proceedings of the CSEE, 2005, 25(11): 107−112 (in Chinese)
10. Ma Hongzhong, Li Xunming, Fang Ruiming, et al. Diagnosis rotor winding fault in asynchronous motors by using residual voltage after AC dump. Proceedings of the CSEE, 2004, 24(7): 183−187 (in Chinese)
11. Zhang Yanxia, Liu Tianxu, Wang Rongqin. Research on the application of Hilbert transformation in micro processor-based Relay protection. Proceedings of the CSEE, 2005, 25(6): 36−41 (in Chinese)
12. Ji Feifeng, Zhou Lidan, Yao Gang, et al. Static var compensator based on the method of synchronous symmetrical component. Proceedings of the CSEE, 2005, 25(6): 24−29 (in Chinese)
13. Lee G M, Lee D C, Seok J K. Control of series active power filters compensating for source voltage unbalance and current harmonics. IEEE Trans. Ind. Electronics, 2004, 51(1): 132−139
14. Ding Hongfa, Duan Xianzhong. Defining instantaneous power components based on the concept of four-dimention complex number. Proceedings of the CSEE, 2003, 23(11): 45−50 (in Chinese)
15. Belling A, Flippest F, et al. Quantitave evaluation of induction motor broken bars by means of electrical signature analysis. IEEE Trans. Ind., 2001, 37(5): 1248−1255
16. Filippetti F, Franceschini G, et al. AI techniques in induction machines diagnosis including the speed ripple effect. IEEE Trans. Ind., 1998, 34(1): 98−108
17. Cruz S M A, Cardoso A J M. Rotor cage fault diagnosis in three-phase induction motors by the total instantaneous power spectral analysis. In: Thirty-Fourth Industry Applications Society Annual Meeting. Coimbra: Portugal, 1999, 3: 1929−1934